Morbid obesity attenuates the skeletal abnormalities associated with leptin deficiency in mice

Russell T Turner[1,2], Kenneth A Philbrick[1], Carmen P Wong[1], Dawn A Olson[1], Adam J Branscum[3] and Urszula T Iwaniec[1,2]

[1]Skeletal Biology Laboratory, School of Biological and Population Health Sciences, [2]Center for Healthy Aging Research and [3]Biostatistics, School of Biological and Population Health Sciences, Oregon State University, Corvallis, Oregon 97331, USA

Correspondence should be addressed to U T Iwaniec
Email
urszula.iwaniec@oregonstate.edu

Abstract

Leptin-deficient *ob/ob* mice are morbidly obese and exhibit low total bone mass and mild osteopetrosis. In order to disassociate the skeletal effects of leptin deficiency from those associated with morbid obesity, we evaluated bone mass, architecture, gene expression, and indices of bone turnover in WT mice, *ob/ob* mice allowed to feed *ad libitum* (*ob/ob*), and *ob/ob* mice pair-fed equivalent to WT mice (pair-fed *ob/ob*). Mice were maintained at 32 °C (thermoneutral) from 6 to 18 weeks of age to minimize differences in resting energy expenditure. *ob/ob* mice were heavier, had more abdominal white adipose tissue (WAT), and were hyperglycemic compared with WT mice. Femur length, bone mineral content (BMC) and bone mineral density, and midshaft femur cortical thickness were lower in *ob/ob* mice than in WT mice. Cancellous bone volume (BV) fraction was higher but indices of bone formation and resorption were lower in *ob/ob* mice compared with WT mice; reduced bone resorption in *ob/ob* mice resulted in pathological retention of calcified cartilage. Pair-fed *ob/ob* mice were lighter and had lower WAT, uterine weight, and serum glucose than *ob/ob* mice. Similarly, femoral length, BMC, and cortical thickness were lower in pair-fed *ob/ob* mice compared with *ob/ob* mice, as were indices of cancellous bone formation and resorption. In contrast, bone marrow adiposity, calcified cartilage, and cancellous BV fraction were higher at one or more cancellous sites in pair-fed *ob/ob* mice compared with *ob/ob* mice. These findings indicate that the skeletal abnormalities caused by leptin deficiency are markedly attenuated in morbidly obese *ob/ob* mice.

Key Words
- obesity
- histomorphometry
- microcomputed tomography
- dual-energy absorptiometry

Journal of Endocrinology (2014) **223**, M1–M15

Introduction

Leptin, a polypeptide hormone secreted by adipocytes, is best known for its role in the regulation of appetite and energy metabolism (Mistry *et al.* 1997, Myers 2004). Rodents deficient in leptin signaling, due to either an inability to generate leptin (*ob/ob* mice) or the signaling form of the leptin receptor (*db/db* mice and *fa/fa* rats), become morbidly obese (Clement 2000). Their excess weight is the result of a combination of hyperphagia and reduced thermogenesis (Hwa *et al.* 1996). In addition to morbid obesity, leptin deficiency is associated with hypogonadism (Barkan *et al.* 2005), elevated corticosteroid levels (Saito & Bray 1983), and impaired thermoregulation (Trayhurn & James 1978).

Leptin-deficient mice and leptin-receptor-deficient mice and rats have reduced overall bone mass, reduced

http://joe.endocrinology-journals.org
DOI: 10.1530/JOE-14-0224

Published by Bioscientifica Ltd.

longitudinal bone growth (Steppan *et al*. 2000, Kishida *et al*. 2005), and decreased bone formation (Gat-Yablonski & Phillip 2008). In addition, impaired bone resorption in *ob/ob* and *db/db* mice results in mild osteopetrosis (Turner *et al*. 2013), a condition that may contribute to the reported reductions in bone quality observed in these animals (Ealey *et al*. 2006, Kimura *et al*. 2012). Impaired bone resorption may also account for the age- and bone-dependent variation in cancellous bone volume (BV) observed in leptin-signaling-deficient mice; the mutant mice have been reported to have normal to increased cancellous BV fraction in lumbar vertebra and decreased to increased cancellous BV fraction in long bones (Hamrick *et al*. 2004, Iwaniec *et al*. 2007, Williams *et al*. 2011). The skeletal abnormalities observed in mice and rats with defective leptin signaling indicate that leptin plays a role in normal skeletal growth, maturation, and turnover (Steppan *et al*. 2000, Kishida *et al*. 2005, Iwaniec *et al*. 2007, Bartell *et al*. 2011, Turner *et al*. 2013). However, it is not clear to what extent the skeletal phenotype of *ob/ob* mice is affected by additional factors associated with morbid obesity.

Although rare in humans, leptin signaling deficiency occurs as a result of loss-of-function mutations in the genes for leptin and the leptin receptor (Friedman & Halaas 1998). More common causes for low levels of leptin signaling in humans include anorexia and starvation (Muller *et al*. 2009, Dardeno *et al*. 2010). At the other end of the spectrum, diet-induced leptin resistance, associated with chronically elevated leptin levels, mimics many of the metabolic consequences of leptin deficiency on energy metabolism and is thought to contribute to the development of morbid obesity (Jung & Kim 2013). Thus, changes in leptin levels and/or leptin sensitivity could have physiological effects on bone metabolism.

In order to better understand the specific actions of leptin in regulating bone mass, density, and architecture, we performed a study in which differences in body weight gain between rapidly growing WT and *ob/ob* mice were prevented by housing all mice at thermoneutral temperature (32 °C) to minimize differences in resting energy expenditure (Trayhurn 1979) and pair-feeding the mutant mice to the level for WT mice to equalize food intake.

Materials and methods

Experimental design

The experimental protocols were approved by the Institutional Animal Care and Use Committee in accordance with the NIH Guide for the Care and Use of Laboratory Animals. Four-week-old female *ob/ob* ($n=20$) and homozygous WT (+/+) littermate ($n=11$) mice were purchased from Jackson Laboratory (Bar Harbor, ME, USA). At 6 weeks of age, all animals were transferred from normal room temperature (22 °C) to thermoneutral temperature (32 °C) and maintained at thermoneutrality on a 12 h light:12 h darkness cycle for the duration of the study (12 weeks). Feed (Teklad 8604, Harlen Laboratories, Indianapolis, IN, USA) and water were provided to WT mice ($n=11$) and a group of *ob/ob* mice ($n=10$) that were allowed to eat and drink *ad libitum*. A second group of *ob/ob* mice ($n=10$) were pair-fed to the WT mice; the *ob/ob* mice were fed an amount of food equivalent to the group mean for WT mice.

Feed consumption was measured daily in WT mice and weekly in *ob/ob* mice allowed to feed *ad libitum*. Body weight was recorded weekly for all mice. The fluorochrome declomycin (20 mg/kg, Sigma) was administered at initiation of the study and the fluorochrome calcein (20 mg/kg, Sigma) was administered 4 days and 1 day before killing to label the mineralizing bone. All mice were fasted overnight. Mice were then anesthetized with 2–3% isoflurane delivered in oxygen, bled by cardiac puncture, and glucose measured using a glucometer (Life Scan, Inc., Milpitas, CA, USA). Serum was collected and stored at −80 °C for measurement of global markers of bone turnover. Uteri and abdominal white adipose tissue (WAT) were excised and weighed. Femora and lumbar vertebrae were removed and stored in 70% ethanol for analysis using dual-energy X-ray absorptiometry (DXA), microcomputed tomography (μCT), and histomorphometry. Tibiae were removed, cleaned of soft tissue, frozen in liquid nitrogen, and stored at −80 °C for mRNA isolation and gene expression analysis.

Serum chemistry

Serum osteocalcin was measured using a mouse Gla-osteocalcin High Sensitive EIA kit obtained from Clontech. Serum CTx was measured using a mouse CTx ELISA kit obtained from Life Sciences Advanced Technologies.

Dual-energy X-ray absorptiometry

Femoral bone mineral content (BMC, mg), area (cm^2), and bone mineral density (BMD, g/cm^2) were determined *ex vivo* using DXA (Piximus, Lunar Corp., Madison, WI, USA).

http://joe.endocrinology-journals.org
DOI: 10.1530/JOE-14-0224

Published by Bioscientifica Ltd.

Microcomputed tomography

Nondestructive three-dimensional evaluation of bone microarchitecture was carried out using μCT (Bouxsein *et al.* 2010). Femora and lumbar vertebrae were scanned in 70% ethanol using a Scanco μCT40 scanner (Scanco Medical AG, Basserdorf, Switzerland) at a voxel size of 12×12×12 μm (55 kV_p X-ray voltage, 145 μA intensity, and 200 ms integration time). Evaluations were carried out with the filtering parameters sigma and support set at 0.8 and 1 respectively. Bone segmentation was carried out at a threshold of 245 (scale, 0–1000) determined empirically. Total femur was evaluated followed by the evaluation of cortical bone in the midshaft femur and cancellous bone in the distal femur metaphysis and epiphysis. Automated contouring was used to delineate cortical bone from non-bone. Then, all cortical slices were examined visually for potential inclusion of cancellous struts originating from the endocortex (extremely rare at this site) and were manually removed when present. For cortical bone, 20 slices (0.24 mm) of bone were evaluated, and cross-sectional tissue volume (TV) (cortical and marrow volume, mm^3), cortical volume (mm^3), marrow volume (mm^3), and cortical thickness (μm) were measured. The polar moment of inertia was determined as a surrogate measure of bone strength in torsion. Architectural parameters are expressed using the standard three-dimensional nomenclature. For the femoral metaphysis, 40 slices (0.48 mm) of cancellous bone were evaluated. The entire cancellous compartment was assessed in the femoral epiphysis. Analysis of lumbar vertebra included the entire region of cancellous bone between the cranial and caudal growth plates. Manual contouring was used to delineate cancellous from cortical bone in the femur metaphysis, femur epiphysis, and vertebral body. Cancellous bone measurements in femur and lumbar vertebra included BV fraction (BV/TV, %), connectivity density (per mm^3), trabecular number (per mm), trabecular thickness (μm), and trabecular separation (μm) (Thomsen *et al.* 2005).

Histomorphometry

The histological methods used here have been described in detail previously (Iwaniec *et al.* 2008). In brief, the distal femur was dehydrated in a graded series of ethanol and xylene and embedded undecalcified in modified methyl methacrylate. Sections (4 μm thick) were cut with a vertical bed microtome (Leica/Jung 2165) and affixed to slides precoated with a 1% gelatin solution. Sections were mounted unstained for the measurement of fluorochrome labels. For cell-based measurements, sections were stained for tartrate-resistant acid phosphatase and counterstained with toluidine blue (Sigma). All data were collected using the OsteoMeasure System (OsteoMetrics, Inc., Atlanta, GA, USA). The sampling site for the distal femoral metaphysis was located 0.25–1.25 mm proximal to the growth plate. The entire cancellous compartment was evaluated in the distal femoral epiphysis and body of lumbar vertebra.

Fluorochrome-based measurements of bone formation included the following parameters: i) mineralizing perimeter (mineralizing perimeter/bone perimeter: cancellous bone perimeter covered with double plus half single label normalized to bone perimeter, %), ii) mineral apposition rate (the distance between two fluorochrome markers that comprise a double label divided by the 3 day interlabel interval, μm/day), and iii) bone formation rate (bone formation rate/bone perimeter: calculated by multiplying mineralizing perimeter by mineral apposition rate normalized to bone perimeter, $μm^2/μm$ per year).

Declomycin label retained in the regions of interest (mm label/mm^2 tissue area) in the distal femur epiphysis and lumbar vertebra was measured as a dynamic index of bone resorption in *ob/ob* and pair-fed *ob/ob* mice. This method is based on the principle that declomycin label was incorporated into bone at equivalent rates in both groups of *ob/ob* mice when the fluorochrome was administered before treatment initiation and differences measured at study termination reflect the effect of treatment on resorption of the fluorochrome-labeled bone. This method has been described previously (Westerlind *et al.* 1997). We did not measure declomycin label in WT mice because almost no label was retained in this group at the termination of the study.

Cell-based measurements included osteoblast perimeter, osteoclast perimeter, adipocyte number, and adipocyte area. Osteoblast perimeter was determined as a percentage of total bone perimeter lined by a palisade of plump cuboidal cells located immediately adjacent to the thin layer of osteoid in direct physical contact with the bone perimeter (osteoblast perimeter/bone perimeter, %). Osteoclast perimeter was determined as the percentage of cancellous bone perimeter covered by multinucleated (two or more nuclei) cells with the acid phosphatase-positive (red-stained) cytoplasm (osteoclast perimeter/bone perimeter, %). Cartilage area in the distal femur metaphysis and epiphysis was measured and expressed as a percentage of the cancellous bone area. The intense metachromatic (purple) staining of proteoglycans and

http://joe.endocrinology-journals.org
DOI: 10.1530/JOE-14-0224

Published by Bioscientifica Ltd.

glycosaminoglycans with toluidine blue was used to identify the cartilage within trabeculae. Adipocyte number and area were also measured and expressed as bone marrow adiposity (tissue area occupied by adipocytes: adipocyte area/tissue area, %), and adipocyte density (number of adipocytes/mm^2). Adipocytes were identified morphologically as large (>75 μm^2) circular or oval-shaped cells bordered by a prominent cell membrane lacking cytoplasmic staining due to alcohol extraction of intracellular lipids during processing. This method has been previously validated by fat extraction and analysis (Menagh *et al*. 2010). All histomorphometric data are expressed using the standard two-dimensional nomenclature (Dempster *et al*. 2013) to distinguish two-dimensional histomorphometric measurements from three-dimensional μCT measurements.

Gene expression

Tibiae were pulverized with a mortar and pestle in liquid nitrogen and then further homogenized in Trizol (Invitrogen). Total RNA was isolated according to the manufacturer's protocol, and mRNA was reverse transcribed into cDNA using SuperScript III First-Strand Synthesis SuperMix for qRT-PCR (Invitrogen). The expression of 84 genes related to osteogenic differentiation was determined using the Mouse Osteogenesis RT^2 Profiler PCR Array (Qiagen) according to the manufacturer's protocol. Gene expression was normalized to *Gapdh* and relative quantification was determined by the ΔΔCt method using RT^2 Profiler PCR Array Data Analysis software version 3.5 (Qiagen).

Statistical analysis

Mean responses for individual variables were compared among the WT, *ob/ob*, and pair-fed *ob/ob* groups using separate one-way ANOVA, with Tukey's procedure for pairwise multiple comparisons. The required conditions for the valid use of ANOVA models were assessed using Levene's test for homogeneity of variance, plots of residuals versus fitted values, normal quantile plots, and the Anderson–Darling test of normality. A modified *F* test was used when the assumption of equal variance was violated, with Welch's two-sample *t*-test used for pairwise comparisons (Welch 1951). The Kruskal–Wallis nonparametric test was used when only the normality assumption was violated, in which case the Wilcoxon–Mann–Whitney test was used for pairwise comparisons. Longitudinal data on body weight were analyzed using a random intercept linear mixed model that allowed distinct linear rates of change for the WT and pair-fed *ob/ob* groups and a quadratic time trend for the *ob/ob* group. The Hommel method for maintaining the familywise error rate at 5% was used to adjust for multiple comparisons (Hommel 1988). Data analysis was performed using R version 2.12. Gene expression analysis was performed using RT^2 Profiler PCR Array Data Analysis version 3.5 (Qiagen). Gene expression is reported as mean fold change. All other data are expressed as mean ± S.E.M.

Results

The effects of pair-feeding (to match food intake in WT mice) on body weight and cumulative food intake, and on abdominal WAT weight, blood glucose levels, uterine weight, and serum osteocalcin and CTx levels at killing in leptin-deficient *ob/ob* mice housed at thermoneutral temperature are shown in Fig. 1. Six-week-old *ob/ob* mice were heavier than their age-matched WT littermates at the start of treatment and gained more weight than WT mice during the 12-week study period (Fig. 1A and B). *ob/ob* mice were hyperphagic consuming, on average, twice as much feed as WT mice (Fig. 1C). At termination of study, the *ob/ob* mice had more abdominal WAT (Fig. 1D) and were hyperglycemic (Fig. 1E) and hypogonadal (Fig. 1F) compared with WT mice.

Pair-fed *ob/ob* mice had a lower body weight and body weight gain, lower cumulative food intake, lower abdominal WAT weight, lower blood glucose levels, and slightly lower uterine weight than *ob/ob* mice. Pair-feeding abolished differences in weight gain and blood glucose levels between WT and *ob/ob* mice. However, the pair-fed *ob/ob* mice were still heavier, had more WAT, and were hypogonadal compared with WT mice.

Effects of pair-feeding on serum markers of bone turnover in *ob/ob* mice

Serum levels of osteocalcin (Fig. 1G) and CTx (Fig. 1H) were lower in *ob/ob* mice than in WT mice. Pair-fed *ob/ob* mice also had lower serum osteocalcin levels than either WT or *ob/ob* mice. Insufficient serum was available for the measurement of CTx in pair-fed *ob/ob* mice.

Effects of pair-feeding on bone mass and architecture in *ob/ob* mice

The effects of pair-feeding on femur BMC, area and BMD, and on femur length, BV, and cortical and cancellous bone

http://joe.endocrinology-journals.org
DOI: 10.1530/JOE-14-0224

Published by Bioscientifica Ltd.

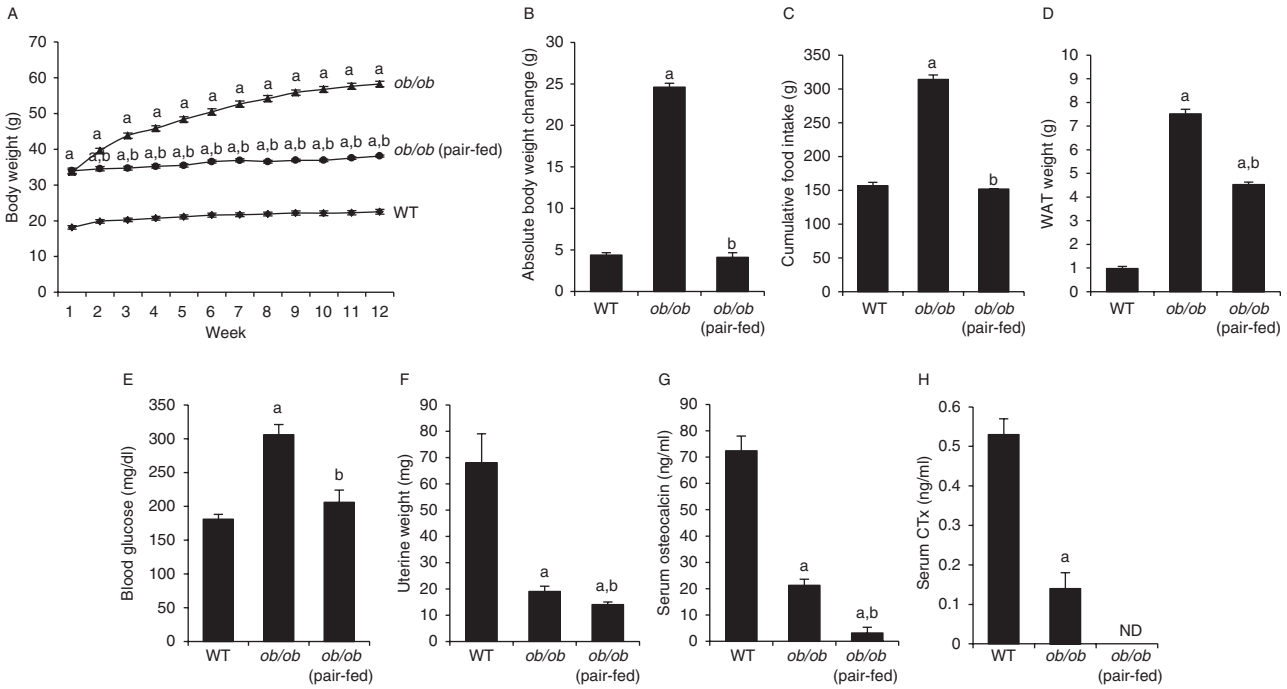

Figure 1
Effects of morbid obesity on body weight (A), cumulative body weight change (B), cumulative food intake (C), abdominal white adipose tissue (WAT) weight (D), blood glucose (E), uterine weight (F), and serum osteocalcin (G) and CTx levels (H) in leptin-deficient *ob/ob* mice.

Values are expressed as mean ± S.E.M., $n = 10–11$/group. ND, no data due to insufficient serum for measurement of CTx in pair-fed *ob/ob* mice. [a]Different from WT mice, $P < 0.05$. [b]Different from *ob/ob* mice, $P < 0.05$.

architecture in *ob/ob* mice are given in Table 1. *ob/ob* mice had lower femur BMC, bone area, and BMD than WT mice. Pair-fed *ob/ob* mice had lower BMC and bone area than WT or *ob/ob* mice. Significant differences in BMD were not detected between *ob/ob* and pair-fed *ob/ob* mice.

Femur length and BV *ob/ob* mice had shorter femurs and a lower femoral BV than WT mice. Pair-fed *ob/ob* mice had a lower femur length and a lower total femur BV than WT or *ob/ob* mice.

Cortical bone in midshaft femur *ob/ob* mice had lower cortical BV and cortical thickness than WT mice. Pair-fed *ob/ob* mice had lower midshaft femur cortical BV and cortical thickness, and greater marrow volume than WT or *ob/ob* mice. Significant differences in cross-sectional volume and polar moment of inertia were not detected among groups.

Cancellous bone in distal femur metaphysis *ob/ob* mice had higher cancellous BV fraction, connectivity density, and trabecular number, and lower trabecular separation than WT mice. Differences in trabecular thickness were not detected between the two groups. Pair-fed *ob/ob* mice had higher cancellous BV fraction and trabecular number, and lower trabecular separation than WT mice or *ob/ob* mice, and a higher connectivity density than WT mice. Trabecular thickness in pair-fed *ob/ob* mice was higher than that in *ob/ob* mice but did not differ from that in WT mice.

Cancellous bone in distal femur epiphysis *ob/ob* mice and pair-fed *ob/ob* mice had higher BV fraction, connectivity density, and trabecular number, and lower trabecular thickness and separation than WT mice. Differences between *ob/ob* mice and pair-fed *ob/ob* mice were not detected for any epiphyseal endpoint measured.

Cancellous bone in lumbar vertebra The effects of pair-feeding on cancellous bone mass and architecture in lumbar vertebra in *ob/ob* mice are given in Table 1. *ob/ob* mice had higher cancellous BV fraction, connectivity density, and trabecular number, and lower trabecular separation than WT mice. Pair-fed *ob/ob* mice had a higher BV fraction than WT mice and a tendency ($P < 0.1$) towards a higher BV fraction than *ob/ob* mice. Pair-fed

http://joe.endocrinology-journals.org
DOI: 10.1530/JOE-14-0224

Published by Bioscientifica Ltd.

Table 1 Effects of morbid obesity on femoral bone mineral content and density, femoral cortical and cancellous bone microarchitecture, and vertebral cancellous bone microarchitecture in leptin-deficient *ob/ob* mice

End point	WT	*ob/ob*	*ob/ob* (pair-fed)	ANOVA *P*[a]
Dual-energy X-ray absorptiometry				
Total femur				
BMC (g)	0.023±0.000	0.019±0.000[b]	0.017±0.000[b,c]	0.0001
Bone area (cm^2)	0.43±0.01	0.40±0.00[b]	0.37±0.01[b,c]	0.0001
BMD (g/cm^2)	0.053±0.001	0.048±0.000[b]	0.047±0.000[b]	0.0003
Microcomputed tomography				
Total femur				
Length (mm)	14.9±0.1	14.2±0.1[b]	13.4±0.1[b,c]	<0.0001
Bone volume (mm^3)	18.5±0.3	16.8±0.3[b]	15.0±0.3[b,c]	<0.0001
Midshaft femur (cortical bone)				
Cross-sectional volume (mm^3)	0.41±0.01	0.40±0.01	0.42±0.01	0.4220
Cortical volume (mm^3)	0.20±0.00	0.18±0.00[b]	0.17±0.00[b,c]	0.0008
Marrow volume (mm^3)	0.22±0.00	0.23±0.00	0.25±0.01[b,c]	0.0012
Cortical thickness (μm)	195±3	176±3[b]	159±2[b,c]	0.0001
Polar moment of inertia (mm^4)	0.36±0.01	0.33±0.01	0.33±0.01	0.4220
Distal femur metaphysis (cancellous bone)				
Bone volume/tissue volume (%)	11.2±0.8	13.2±0.5[b]	18.1±0.5[b,c]	0.0004
Connectivity density ($1/mm^3$)	106±9	173±7[b]	190±8[b]	<0.0001
Trabecular thickness (μm)	44±1	41±1	45±0[c]	0.0365
Trabecular number (per mm)	4.8±0.1	5.2±0.1[b]	5.7±0.1[b,c]	0.0001
Trabecular separation (μm)	210±4	191±4[b]	173±4[b,c]	0.0013
Distal femur epiphysis (cancellous bone)				
Bone volume/tissue volume (%)	31.2±0.6	36.1±0.6[b]	36.6±0.9[b]	0.0013
Connectivity density ($1/mm^3$)	155±4	254±8[b]	261±7[b]	<0.0001
Trabecular thickness (μm)	64±1	60±1[b]	58±1[b]	0.0001
Trabecular number (per mm)	5.5±0.1	6.7±0.1[b]	6.7±0.1[b]	0.0004
Trabecular separation (μm)	179±2	138±3[b]	138±3[b]	<0.0001
Lumbar vertebra (cancellous bone)				
Bone volume/tissue volume (%)	21.8±1.0	31.5±0.8[b]	34.2±0.5[b]	<0.0001
Connectivity density ($1/mm^3$)	198±10	364±15[b]	191±5[c]	<0.0001
Trabecular thickness (μm)	49±1	50±0.5	54±0.4[b,c]	0.0010
Trabecular number (per mm)	4.6±0.1	6.0±0.1[b]	5.8±0.1[b]	0.0004
Trabecular separation (μm)	215±5	160±3[b]	163±3[b]	0.0005

[a]The Hommel method for maintaining the familywise error rate at 5% was used to adjust for multiple comparisons.
[b]Different from WT, $P<0.05$.
[c]Different from *ob/ob*, $P<0.05$.

ob/ob mice also had higher trabecular thickness than WT or *ob/ob* mice. Connectivity density was lower in pair-fed *ob/ob* mice than in *ob/ob* mice but did not differ from that for WT mice. Trabecular number was higher and trabecular separation was lower in pair-fed *ob/ob* mice than WT mice. Differences in trabecular number and separation were not detected between *ob/ob* mice and pair-fed *ob/ob* mice.

Effects of pair-feeding on bone histomorphometry in *ob/ob* mice

Cancellous bone in distal femur metaphysis The effects of pair-feeding on dynamic and static cancellous bone histomorphometry and marrow adiposity in the distal femur metaphysis in *ob/ob* mice are shown in Fig. 2. *ob/ob* mice had lower mineralizing perimeter (Fig. 2A), mineral apposition rate (Fig. 2B), bone formation rate (Fig. 2C), and osteoblast perimeter (Fig. 2D) compared with WT mice. Pair-fed *ob/ob* mice had lower mineralizing perimeter, mineral apposition rate, bone formation rate, and osteoblast perimeter than WT or *ob/ob* mice. Differences in osteoclast perimeter (Fig. 2E) were not detected with treatment. However, cartilage area (Fig. 2F), an index of impaired bone resorption, was higher in both groups of *ob/ob* mice compared with WT mice. Bone marrow adiposity (Fig. 2G) tended ($P<0.1$) to be greater in *ob/ob* mice than WT mice and was greater in pair-fed *ob/ob* mice than in WT or *ob/ob* mice. Adipocyte density (Fig. 2H) was higher in pair-fed *ob/ob* mice than in *ob/ob* mice. Representative photomicrographs of marrow adipocytes in the three groups of mice are shown in Fig. 3A, B and C.

http://joe.endocrinology-journals.org
DOI: 10.1530/JOE-14-0224

Published by Bioscientifica Ltd.

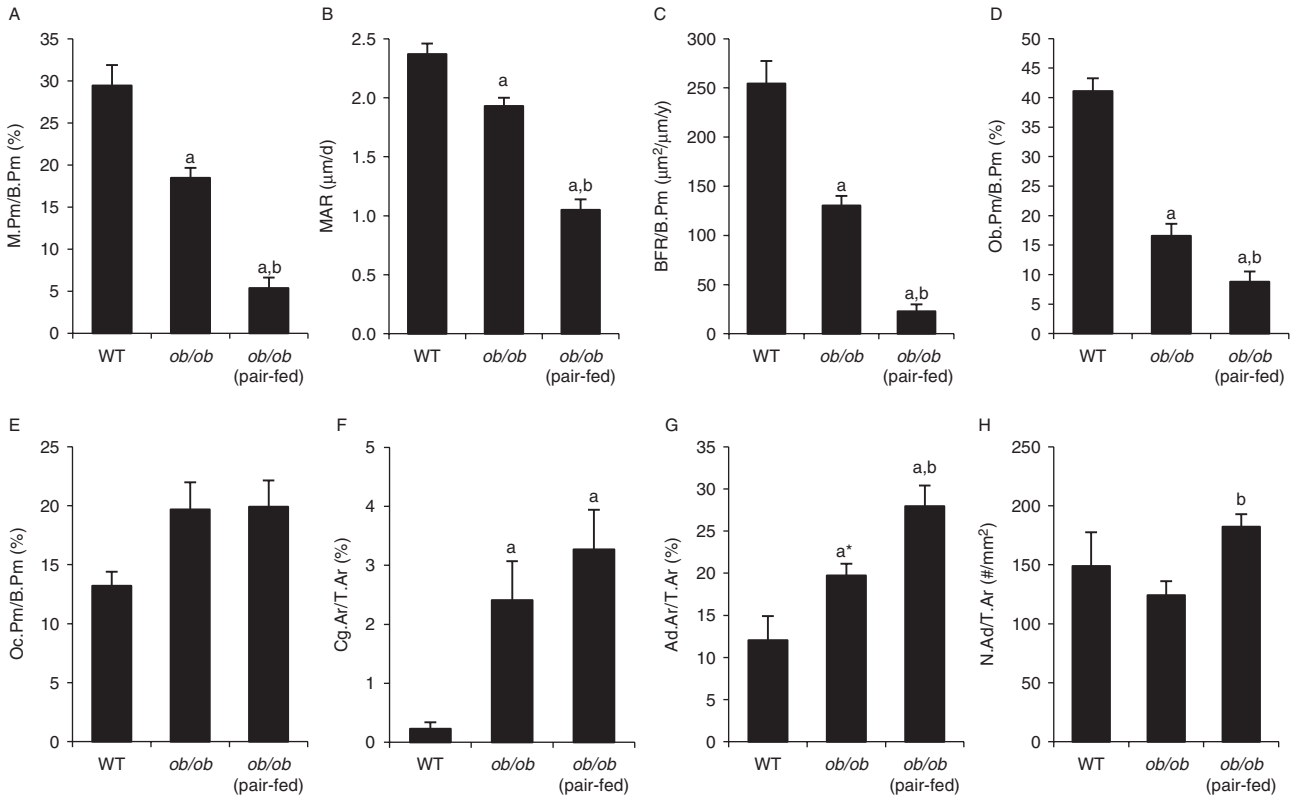

Figure 2
Effects of morbid obesity on cancellous bone histomorphometry and marrow adiposity in distal femur metaphysis in leptin-deficient *ob/ob* mice. Shown are mineralizing perimeter (A, mineralizing perimeter/bone perimeter, M.Pm/B.Pm), mineral apposition rate (B, MAR), bone formation rate (C, bone formation rate/bone perimeter, BFR/B.Pm), osteoblast perimeter (D, osteoblast perimeter/bone perimeter, Ob.Pm/B.Pm), osteoclast perimeter (E, osteoclast perimeter/bone perimeter, Oc.Pm/B.Pm), cartilage area (F, cartilage area/tissue area, Cg.Ar/T.Ar), marrow adiposity (G, adipocyte area/tissue area, Ad.Ar/T.Ar), and adipocyte density (H, number of adipocytes/tissue area, N.Ad/T.Ar). Values are expressed as mean ± S.E.M., $n = 10–11$/group. [a]Different from WT mice, $P < 0.05$. [a*]Different from WT mice, $P < 0.1$. [b]Different from *ob/ob* mice, $P < 0.05$.

Cancellous bone in distal femur epiphysis The effects of pair-feeding on dynamic and static cancellous bone histomorphometry and marrow adiposity in the distal femur epiphysis in *ob/ob* mice are shown in Fig. 4. *ob/ob* mice had lower mineralizing perimeter (Fig. 4A), bone formation rate (Fig. 4C), and osteoblast perimeter (Fig. 4D) than WT mice. Pair-fed *ob/ob* mice had lower mineralizing perimeter, bone formation rate, and osteoblast perimeter than WT or *ob/ob* mice. Osteoclast perimeter (Fig. 4E) was higher in *ob/ob* mice and pair-fed *ob/ob* mice than in WT mice. Retention of declomycin label (Fig. 4F), an index of decreased bone resorption, was higher in pair-fed *ob/ob* mice than in *ob/ob* mice. *ob/ob* mice had greater cartilage area (Fig. 4G), marrow adiposity (Fig. 4H), and adipocyte density (Fig. 4I) than WT mice. Pair-fed *ob/ob* mice had higher cartilage area, marrow adiposity, and adipocyte density than WT or *ob/ob* mice. Representative photomicrographs showing cartilage and declomycin labelling in the three groups are shown in Fig. 3D, E, F and G, H, I respectively.

Cancellous bone in lumbar vertebra The effects of pair-feeding on dynamic and static cancellous bone histomorphometry and on bone marrow adiposity in lumbar vertebra are shown in Fig. 5. *ob/ob* mice had lower mineralizing perimeter (Fig. 5A), bone formation rate (Fig. 5C), and osteoblast perimeter (Fig. 5D) than WT mice. Pair-fed *ob/ob* mice had lower mineralizing perimeter, mineral apposition rate (Fig. 5B), bone formation rate, and osteoblast perimeter than WT or *ob/ob* mice. Significant differences in osteoclast perimeter (Fig. 5E) were not detected among the three groups. However, retention of declomycin label (Fig. 5F) was higher in pair-fed *ob/ob* mice than in *ob/ob* mice. *ob/ob* mice had greater marrow

http://joe.endocrinology-journals.org
DOI: 10.1530/JOE-14-0224

Published by Bioscientifica Ltd.

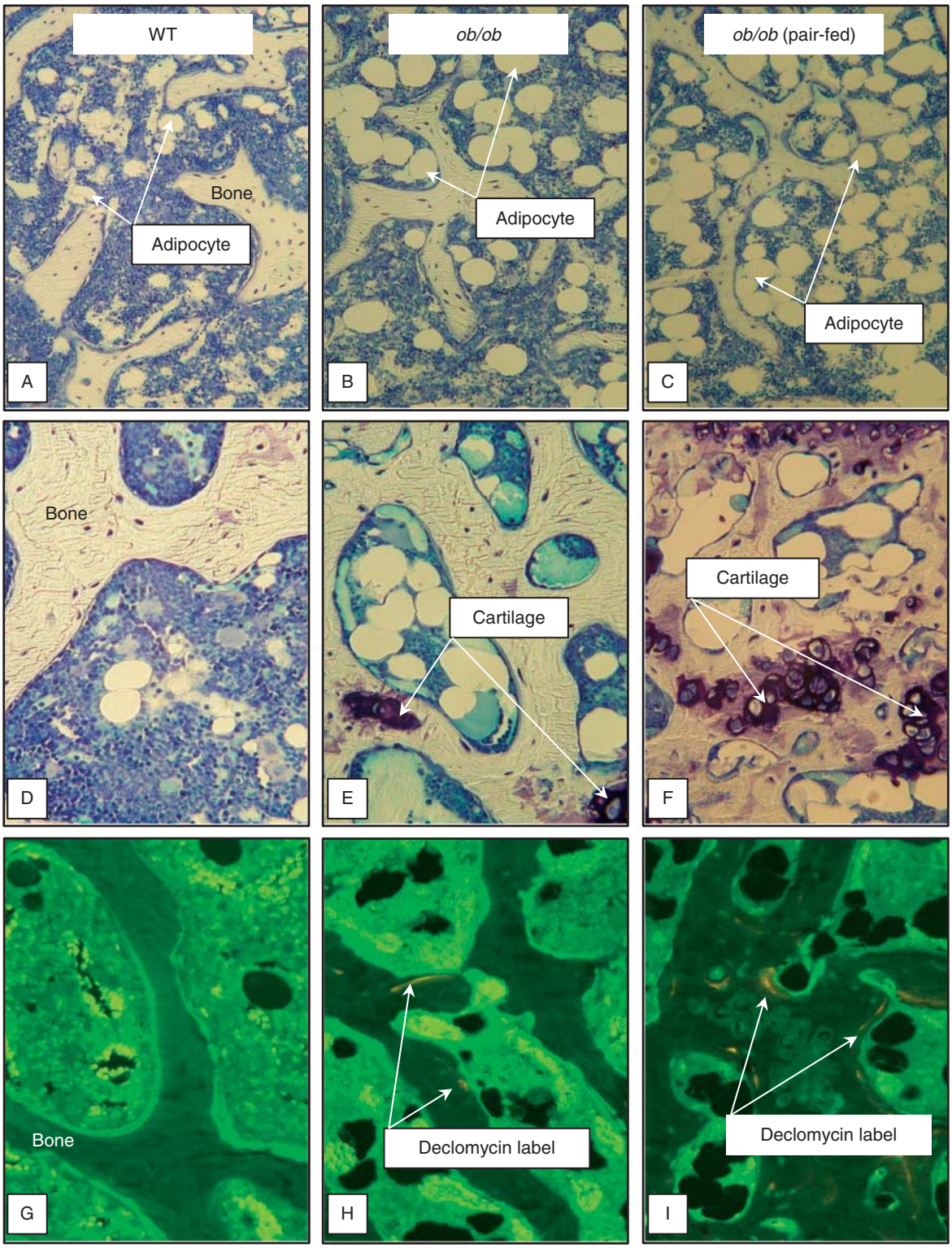

Figure 3
Representative photomicrographs of i) marrow adiposity in distal femur metaphysis in WT mouse (A), *ob/ob* mouse (B), and pair-fed *ob/ob* mouse (C), ii) cartilage remnants in distal femur epiphysis in WT mouse (D), *ob/ob* mouse (E), and pair-fed *ob/ob* mouse (F), and iii) declomycin label administered at study initiation in distal femur epiphysis in WT mouse (G), *ob/ob* mouse (H), and pair-fed *ob/ob* mouse (I).

http://joe.endocrinology-journals.org
DOI: 10.1530/JOE-14-0224

Published by Bioscientifica Ltd.

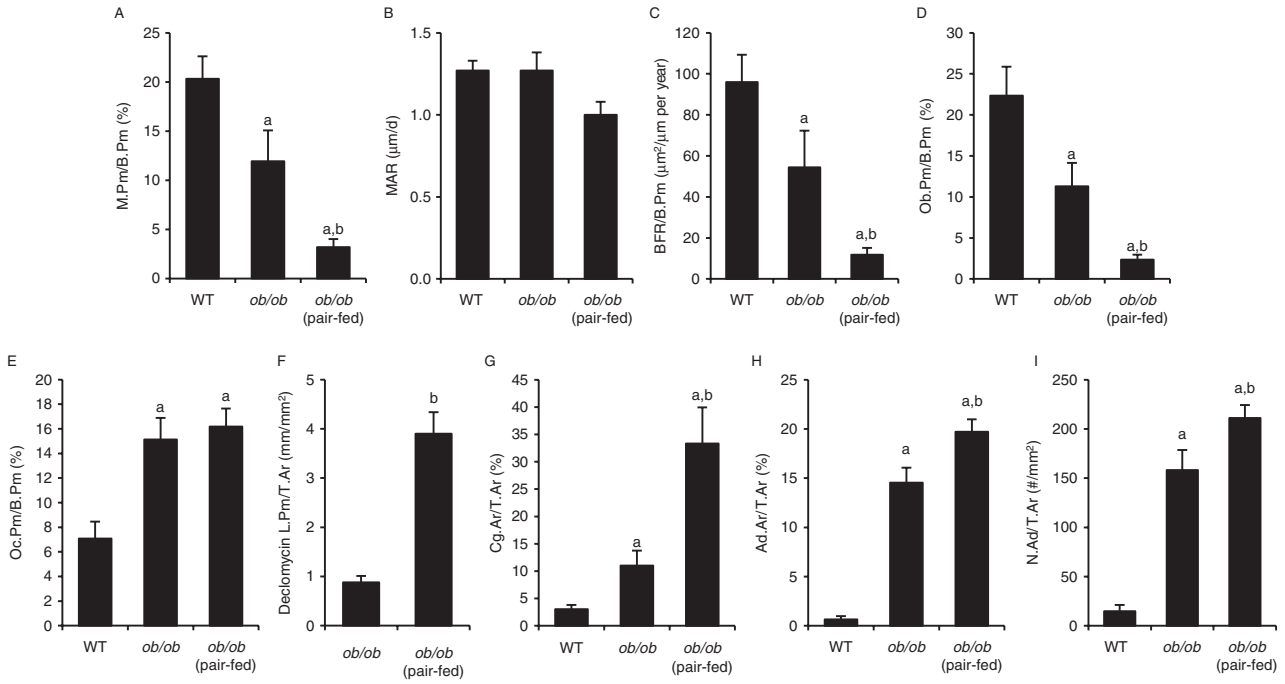

Figure 4
Effects of morbid obesity on cancellous bone histomorphometry and marrow adiposity in distal femur epiphysis in leptin-deficient *ob/ob* mice. Shown are mineralizing perimeter (A, mineralizing perimeter/bone perimeter, M.Pm/B.Pm), mineral apposition rate (B, MAR), bone formation rate (C, bone formation rate/bone perimeter, BFR/B.Pm), osteoblast perimeter (D, osteoblast perimeter/bone perimeter, Ob.Pm/B.Pm), osteoclast perimeter (E, osteoclast perimeter/bone perimeter, Oc.Pm/B.Pm), declomycin label perimeter (F, declomycin label perimeter/tissue area, declomycin L.Pm/T.Ar), cartilage area (G, cartilage area/tissue area, Cg.Ar/T.Ar), marrow adiposity (H, adipocyte area/tissue area, Ad.Ar/T.Ar), and adipocyte density (I, number of adipocytes/tissue area, N.Ad/T.Ar). Values are mean ± S.E.M., $n = 10$–11/group. [a]Different from WT mice, $P < 0.05$. [b]Different from *ob/ob* mice, $P < 0.05$.

adiposity (Fig. 5G) and adipocyte density (Fig. 5H) than WT mice. Pair-fed *ob/ob* mice had higher marrow adiposity and adipocyte density than WT or *ob/ob* mice.

Effects of pair-feeding on gene expression in tibia

The effects of pair-feeding on expression of 84 genes related to osteogenesis in tibia are shown in Fig. 6. Compared with WT mice, expression levels of 24 genes were altered in *ob/ob* mice (seven higher and 17 lower) and 26 genes in pair-fed *ob/ob* mice (ten higher and 16 lower). The expression levels of 14 genes were altered in common in *ob/ob* and pair-fed *ob/ob* mice. Compared with *ob/ob* mice, expression levels of 11 genes (three higher and eight lower) were altered in pair-fed *ob/ob* mice. *ob/ob* mice exhibited reductions in several key genes related to osteoblast and osteoclast differentiation and function, including *Sp7*/osterix (−2.5-fold), *NfkB1* (−1.2-fold), alkaline phosphatase (*Alpl*) (−1.5-fold), *Cd11b* (*Itgam*) (−1.3-fold), and osteocalcin (*Bglap*) (−1.8-fold). *ob/ob* mice also exhibited reductions in genes related to cartilage formation and maturation, including *col2a1* (−1.5-fold) and *col10a1* (−1.7-fold). Genes whose expressions were elevated include *Bmpr1a* (+1.3-fold) and *Smad4* (+1.3-fold). Compared with WT mice, pair-fed *ob/ob* mice expressed even lower levels of osteocalcin (−3.8-fold) than those observed in *ob/ob* mice and, in addition, had lower mRNA levels for the osteoclast differentiation factor *Csf1* (−1.5-fold) and osteoblast differentiation factor *Runx2* (−1.4-fold). Furthermore, compared with WT mice, pair-fed *ob/ob* mice had higher gene expression levels for the cytokines/growth factors *Tnfa* (TNF) (+1.6-fold) and *Tgfb2* (+1.3-fold).

Discussion

We investigated the contribution of excessive weight gain to the skeletal phenotype of leptin-deficient *ob/ob* mice. Mice were housed at 32 °C and a group of *ob/ob* mice was pair-fed to WT mice. Housing mice at 32 °C, which is within the thermoneutral range for WT and *ob/ob* mice, was expected to minimize the differences in the resting energy expenditure and pair-feeding *ob/ob* mice with respect to WT mice was expected to equalize energy intake

http://joe.endocrinology-journals.org
DOI: 10.1530/JOE-14-0224

Published by Bioscientifica Ltd.

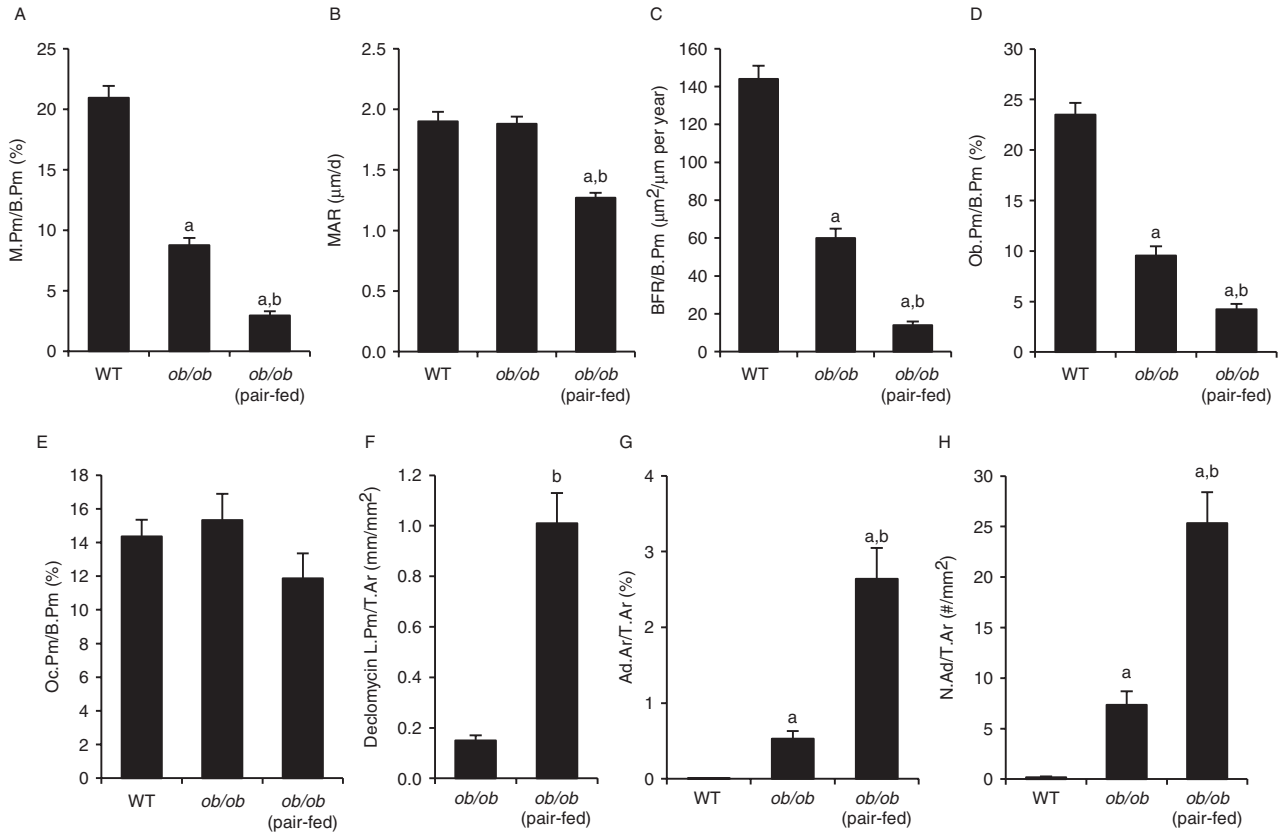

Figure 5
Effects of morbid obesity on cancellous bone histomorphometry and marrow adiposity in lumbar vertebra in leptin-deficient *ob/ob* mice. Shown are mineralizing perimeter (A, mineralizing perimeter/bone perimeter, M.Pm/B.Pm), mineral apposition rate (B, MAR), bone formation rate (C, bone formation rate/bone perimeter, BFR/B.Pm), osteoblast perimeter (D, osteoblast perimeter/bone perimeter, Ob.Pm/B.Pm), osteoclast perimeter (E, osteoclast perimeter/bone perimeter, Oc.Pm/B.Pm), declomycin label perimeter (F, declomycin label perimeter/tissue area, declomycin L.Pm/T.Ar), marrow adiposity (G, adipocyte area/tissue area, Ad.Ar/T.Ar), and adipocyte density (H, number of adipocytes/tissue area, N.Ad/T.Ar). Values are expressed as mean ± S.E.M., $n = 10–11$/group. [a]Different from WT mice, $P < 0.05$. [b]Different from *ob/ob* mice, $P < 0.05$.

(Knehans & Romsos 1982, Rafael & Herling 2000). The parallel increase in body weight gain in WT mice and *ob/ob* mice pair-fed with respect to WT mice over the 12-week duration of study demonstrates the efficacy of this approach for preventing the development of morbid obesity in leptin-deficient mice.

Consistent with results from earlier studies (Hamrick *et al*. 2004, Ealey *et al*. 2006, Iwaniec *et al*. 2007, Williams *et al*. 2011), *ob/ob* mice exhibited a mosaic skeletal phenotype associated with decreased bone formation due to reduced osteoblast number and activity, and defective osteoclast function. Femurs from *ob/ob* mice were smaller and had thinner cortices than those from WT mice. Furthermore, serum osteocalcin levels, mRNA levels of osteocalcin and *Sp7* (osterix), osteoblast perimeter, and dynamic indices of bone formation were lower in *ob/ob* mice than in WT mice. However, cancellous BV fraction in both distal femur and lumbar vertebra was higher in the *ob/ob* mice. The higher cancellous BV fraction was associated with i) greatly reduced serum CTx levels, ii) reductions in mRNA levels of *Nfkb1*, *Itgam*, and *Icam1*, iii) retention of calcified cartilage, and iv) retention of fluorochrome label administered at the start of the study, all indicative of a defect in bone resorption. Osteoclast perimeter was either unaffected (distal femur metaphysis and lumbar vertebra) or increased (distal femur epiphysis), indicating that reduced bone resorption in *ob/ob* mice was not due to an inability to generate osteoclasts. Taken together, these findings further support our previous observation that *ob/ob* mice exhibit mild osteopetrosis. Osteopetrosis due to a defect in osteoclast function may be responsible for the poor bone quality (Ealey *et al*. 2006) and defective tooth eruption (Batt 1978, 1992) reported in *ob/ob* mice.

Pair-feeding accentuated many of the abnormalities in bone size, mass, microarchitecture, gene expression,

http://joe.endocrinology-journals.org
DOI: 10.1530/JOE-14-0224

Published by Bioscientifica Ltd.

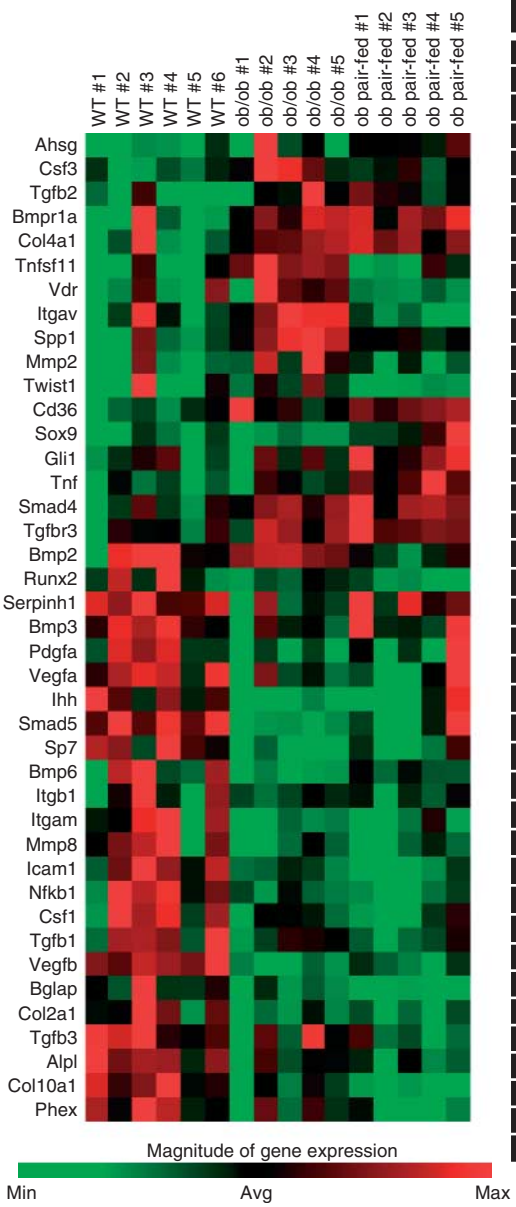

Symbol	*ob/ob*	*ob/ob* (pair-fed)
Ahsg	1.3	1.5[a]
Alpl	−1.5[a]	−1.6[a]
Bglap	−1.8[a]	−3.8[a,b]
Bmp2	1.1	−1.1[b]
Bmp3	−1.4[a]	−1.1
Bmp6	−1.4[a]	−1.1[b]
Bmpr1a	1.3[a]	1.3[a]
Cd36	1.4	1.6[a]
Col10a1	−1.7[a]	−3.0[a,b]
Col2a1	−1.5[a]	−1.5[a]
Col4a1	1.2	1.3[a]
Csf1	−1.3	−1.5[a]
Csf3	1.6[a]	1.3
Gli1	1.0	1.3[a]
Icam1	−1.3[a]	−1.5[a]
Ihh	−2.7[a]	−1.9
Itgam	−1.3[a]	−1.3[a]
Itgav	1.3[a]	−1.1[b]
Mmp2	1.4[a]	1.1
Mmp8	−1.4[a]	−1.4[a]
Nfkb1	−1.2[a]	−1.4[a]
Pdgfa	−1.4[a]	−1.2
Phex	−1.3	−1.6[a]
Runx2	−1.1	−1.4[a]
Serpinh1	−1.6[a]	−1.1
Smad4	1.3[a]	1.4[a]
Smad5	−1.7[a]	−1.4[a]
Sox9	−1.1	1.5[a,b]
Sp7	−2.5[a]	−1.7[a]
Spp1	1.9[a]	1.4[b]
Tgfb1	−1.2	−1.2[a]
Tgfb2	1.2	1.3[a]
Tgfb3	−1.2	−1.3[a]
Tgfbr3	1.3	1.4[a]
Tnfa	1.2	1.6[a,b]
Tnfsf11	2.5[a]	1.3[b]
Twist1	1.4	−1.1[b]
Vdr	1.4	−1.0[b]
Vegfa	−1.2[a]	−1.2
Vegfb	−1.4[a]	−1.3[a]

Figure 6

Effects of morbid obesity on expression of osteogenesis-related genes in tibia. The expressions of a panel of 84 osteogenesis-related genes in the tibia of WT mice ($n=6$), *ob/ob* mice ($n=5$), and *ob/ob* mice pair-fed to the WT mice ($n=5$) were determined using a mouse osteogenesis gene expression array. Left panel shows hierarchical clustering analysis of genes with significantly different gene expression. The magnitude of gene expression was represented by green and red bars, indicating decreased and increased expression respectively. The normalized mean fold change of *ob/ob* mice and pair-fed *ob/ob* mice relative to the WT mice was shown in the right panel. [a]Different from WT mice, $P<0.05$. [b]Different from *ob/ob* mice, $P<0.05$.

and turnover typically observed in *ob/ob* mice. Thus, chronic excessive weight gain typically present in *ob/ob* mice reduces the magnitude of skeletal effects associated with leptin deficiency. We did not adjust μCT-derived cortical bone data for body weight differences because the association between body weight and bone size and density in growing mice varies with bone and bone compartment and this association is altered by leptin (Iwaniec *et al.* 2009). However, it is clear that the weight gain due to hyperphagia in *ob/ob* mice was associated

http://joe.endocrinology-journals.org
DOI: 10.1530/JOE-14-0224

Published by Bioscientifica Ltd.

with increases in cortical bone accrual but that these gains were not commensurate with the magnitude of body weight gain.

The mechanisms for the partial protective effect of morbid obesity on bone in *ob/ob* mice are likely to be multifactorial. We have previously reported a strong positive correlation between body weight and total femur bone mass in *ob/ob* mice (Iwaniec *et al*. 2009). This finding provides strong evidence that the higher total and cortical bone mass in mice allowed to feed *ad libitum* compared with pair-fed *ob/ob* mice are, at least in part, attributable to higher body weight. Although there have been significant recent advances in our understanding of the regulation of bone metabolism by mechanotransduction, the molecular mechanism for this positive effect of weight on bone mass is largely unknown. In addition to direct effects of increased mechanical loading, changes in levels of hormones and/or growth factors may mediate additional effects of increased weight on the skeleton (Robling 2012).

We did not measure the levels of insulin, glucocorticoids, or norepinephrine, factors known to be dysregulated in *ob/ob* mice (Knehans & Romsos 1982, Dubuc *et al*. 1985, Kim & Romsos 1990, Rafael & Herling 2000) and known to influence bone metabolism. However, housing food-restricted *ob/ob* mice at thermoneutral temperature has been reported to reduce abnormalities in blood glucose, insulin, glucocorticoids, and norepinephrine turnover. In contrast, *ob/ob* mice allowed to feed *ad libitum* have been reported to remain hyperglycemic and hyperinsulinemic (Lindstrom 2007). We confirmed that blood glucose levels in pair-fed *ob/ob* mice did not differ from those of WT mice and were much lower than those of *ob/ob* mice allowed to feed *ad libitum*. The contribution of excess insulin secretion and other factors associated with morbid obesity to the protective effects of excess body weight (Martineau-Doize *et al*. 1986, Ituarte *et al*. 1988, Pun *et al*. 1989, Hickman & McElduff 1990, Yaturu 2009) on cortical bone microarchitecture in *ob/ob* mice requires further investigation.

Leptin is required for gonadotropin-releasing hormone secretion (Donato *et al*. 2011). As a consequence, *ob/ob* mice are severely hypogonadal (Chehab *et al*. 2002). The resulting deficiency in sex steroids would be expected to play a role in the pathological skeletal changes associated with leptin deficiency because sex steroids, especially estrogen, contribute to the sexual dimorphism of the female skeleton and regulate bone turnover balance in adults (Turner *et al*. 1989, 1994, Rickard *et al*. 2008). Gonadal dysfunction typically results in elevated bone turnover and cancellous osteopenia. The difference between the skeletal responses to gonadal hormone insufficiency resulting from gonadectomy (high turnover) and from leptin-deficiency (low turnover) is perplexing. However, estrogen has a tonic effect on bone resorption and leptin is required for normal osteoclast function. As a consequence, the high bone turnover generally associated with estrogen deficiency may be attenuated in *ob/ob* mice due to impaired osteoclast function. We speculate that the requirement for leptin in normal osteoclast function may serve as a counter-regulatory mechanism to prevent excessive bone loss during fasting.

We did not measure sex steroid levels but the higher uterine weight in *ob/ob* mice fed *ad libitum* compared with pair-fed *ob/ob* mice implies that morbid obesity results in a small increase in circulating estrogen. Higher estrogen levels in blood or adipose tissue may contribute to the protective skeletal effects of morbid obesity (Turner *et al*. 1994, Turner 1999, Gennari *et al*. 2011). Aromatase, the enzyme responsible for conversion of androgens to estrogens, is expressed by adipocytes (Gennari *et al*. 2011). Thus, adipose-derived estrogen is a plausible factor contributing to the skeletal differences between pair-fed mice and *ob/ob* mice allowed to feed *ad libitum*.

Initially heavier *ob/ob* mice pair-fed with respect to WT mice remained heavier than WT mice during the entire study period. We chose to equalize energy availability rather than body weight in this study, because bone accrual in rapidly growing rodents is strongly associated with energy availability and bone loss accompanies weight loss in adults (Devlin *et al*. 2010, Turner & Iwaniec 2011). Low leptin levels induced by caloric restriction are associated with diminished bone mass accrual, whereas partial leptin signaling deficiency induced in mice allowed to feed *ad libitum* by treatment with a leptin antagonist increased body weight and bone mass accrual (Solomon *et al*. 2014). However, administration of leptin increases bone formation in adult *ob/ob* mice in spite of weight loss (Bartell *et al*. 2011, Turner *et al*. 2013). Thus, both adequate energy availability and leptin play important roles in bone accrual in growing mice.

In contrast to peripheral fat depots, which act as dynamic energy reservoirs to maintain circulating triglyceride and free fatty acid levels during feeding and fasting, marrow fat increases with severe weight loss as well as weight gain (Bredella *et al*. 2011, Devlin 2011). It is therefore unlikely that the bone marrow fat depot serves as an important energy reservoir for peripheral tissues. There is, however, evidence that bone marrow adipocytes function as negative regulators of hematopoietic lineage

http://joe.endocrinology-journals.org
DOI: 10.1530/JOE-14-0224

Published by Bioscientifica Ltd.

cell differentiation (Gimble *et al*. 1996, Dorshkind *et al*. 2009, Naveiras *et al*. 2009). Bone marrow fat is increased in *ob/ob* mice and this increase is reversed by leptin treatment (Hamrick *et al*. 2004, 2005, Bartell *et al*. 2011). Leptin stimulates hematopoiesis (Fantuzzi & Faggioni 2000, Trottier *et al*. 2012), an action that may result from inhibition of bone marrow adipogenesis, increased lipolysis, and direct stimulatory actions on hematopoietic cells. Adipocytes and osteoblasts are derived from the same bone marrow mesenchymal precursor and a reciprocal association between the osteoblast number and the adipocyte number has often been noticed, giving rise to the hypothesis that either bone marrow adipocytes may antagonize osteoblast production or, alternatively, generation of adipocytes may preclude generation of osteoblasts (Akune *et al*. 2004). Results from other studies indicate that the adipocyte and osteoblast number in bone marrow can be independently regulated (Menagh *et al*. 2010, Iwaniec & Turner 2013). Bartell *et al*. (2011) reported that i.c.v. administration of leptin to *ob/ob* mice increases expression of *Sp7*, a transcription factor critical for osteoblast differentiation. Our findings of low expression of SP7 in *ob/ob* mice support the hypothesis that leptin acts to regulate bone formation by controlling mesenchymal cell decision.

In this study, pair-feeding with respect to WT mice resulted in a further increase in bone marrow adiposity in leptin-deficient *ob/ob* mice. Of interest is our finding that pair-fed *ob/ob* mice had elevated mRNA levels of *Cd36*; CD36 (fatty acid translocase) promotes adipocyte differentiation and adipogenesis (Christiaens *et al*. 2012). The observed increase in CD36 may play a role in the increased bone marrow adiposity observed in the pair-fed *ob/ob* mice. Additional factors regulating bone marrow adiposity that may be influenced by leptin levels and obesity include growth hormone and insulin-like growth factor 1 (IGF1). In rats, treatment with parathyroid hormone (whose actions on bone are largely mediated by IGF1) prevented the increase in bone marrow adiposity associated with severe energy restriction (Turner & Iwaniec 2011), whereas growth hormone treatment dramatically reduced excessive bone marrow adiposity in severely hypoleptinemic hypophysectomized rats (Menagh *et al*. 2010). In both of these studies, treatment had no effect on serum leptin levels. *ob/ob* mice, however, have decreased circulating growth hormone and impaired growth hormone signaling (Luque *et al*. 2007), probably contributing to retention of fat within the bone marrow. High circulating insulin levels in morbidly obese *ob/ob* mice may further contribute to the suppression of growth hormone synthesis and release (Luque & Kineman 2006). However, IGF1 is produced and secreted by adipocytes (Kloting *et al*. 2008) and higher levels of IGF1 are detected in obese subjects (Frystyk *et al*. 1999). Low leptin levels resulting from severe energy restriction are associated with increased growth hormone secretion, decreased circulating levels of IGF1, and end-organ resistance to growth hormone (Grinspoon *et al*. 1995, Thissen *et al*. 1999, Douyon & Schteingart 2002, Munoz & Argente 2002, Inagaki *et al*. 2008). Thus, disturbances in growth hormone, IGF1, and insulin signaling as well as leptin deficiency may contribute to the increase in bone marrow adiposity in *ob/ob* mice. Chronic hyperphagia and excessive weight gain typically observed in *ob/ob* mice may partially compensate for leptin deficiency and reduced bone marrow adiposity by altering growth hormone and insulin levels and sensitivity.

In summary, leptin deficiency resulted in decreased femur length, BMC, BMD, and cortical BV and thickness. In contrast, the cancellous BV fraction was increased in distal femur and lumbar vertebra. The profound changes in bone mass, density, and microarchitecture were associated with reduced linear bone growth, increased bone marrow adiposity, altered expression of osteogenic genes, decreased osteoblast number, and decreased osteoclast function. Prevention of morbid obesity in *ob/ob* mice further exacerbated many of the abnormalities associated with leptin deficiency. As morbid obesity normally present in *ob/ob* mice attenuates the abnormal skeletal phenotype associated with leptin deficiency, the role of leptin in regulating postnatal bone growth, maturation, and turnover may have been underestimated.

Declaration of interest

The authors declare that there is no conflict of interest that could be perceived as prejudicing the impartiality of the research reported.

Funding

This work was supported by the National Institutes of Health (NIH) (AR 060913), the National Aeronautics and Space Administration (NASA) (NNX12AL24), and the United States Department of Agriculture (USDA) (38420-17804).

References

Akune T, Ohba S, Kamekura S, Yamaguchi M, Chung UI, Kubota N, Terauchi Y, Harada Y, Azuma Y, Nakamura K *et al*. 2004 PPARγ insufficiency enhances osteogenesis through osteoblast formation from bone marrow progenitors. *Journal of Clinical Investigation* **113** 846–855. (doi:10.1172/JCI200419900)

http://joe.endocrinology-journals.org
DOI: 10.1530/JOE-14-0224

Published by Bioscientifica Ltd.

Barkan D, Hurgin V, Dekel N, Amsterdam A & Rubinstein M 2005 Leptin induces ovulation in GnRH-deficient mice. *FASEB Journal* **19** 133–135. (doi:10.1096/fj.04-2271fje)

Bartell SM, Rayalam S, Ambati S, Gaddam DR, Hartzell DL, Hamrick M, She JX, Della-Fera MA & Baile CA 2011 Central (ICV) leptin injection increases bone formation, bone mineral density, muscle mass, serum IGF-1, and the expression of osteogenic genes in leptin-deficient *ob/ob* mice. *Journal of Bone and Mineral Research* **26** 1710–1720. (doi:10.1002/jbmr.406)

Batt RA 1978 Abnormal dentition and decrease in body weight in the genetically obese mouse (genotype, ob/ob). *International Journal of Obesity* **2** 457–462.

Batt RA 1992 Abnormal incisor teeth and body weight in the obese mouse (genotype ob/ob). *International Journal of Obesity and Related Metabolic Disorders* **16** 29–34.

Bouxsein ML, Boyd SK, Christiansen BA, Guldberg RE, Jepsen KJ & Muller R 2010 Guidelines for assessment of bone microstructure in rodents using micro-computed tomography. *Journal of Bone and Mineral Research* **25** 1468–1486. (doi:10.1002/jbmr.141)

Bredella MA, Torriani M, Ghomi RH, Thomas BJ, Brick DJ, Gerweck AV, Rosen CJ, Klibanski A & Miller KK 2011 Vertebral bone marrow fat is positively associated with visceral fat and inversely associated with IGF-1 in obese women. *Obesity* **19** 49–53. (doi:10.1038/oby.2010.106)

Chehab FF, Qiu J, Mounzih K, Ewart-Toland A & Ogus S 2002 Leptin and reproduction. *Nutrition Reviews* **60** S39–S46 discussion S68-84, 85-37. (doi:10.1301/002966402320634823)

Christiaens V, Van Hul M, Lijnen HR & Scroyen I 2012 CD36 promotes adipocyte differentiation and adipogenesis. *Biochimica et Biophysica Acta* **1820** 949–956. (doi:10.1016/j.bbagen.2012.04.001)

Clement K 2000 Monogenic forms of obesity: from mice to human. *Annales d'Endocrinologie* **61**(Suppl 6) 39–49.

Dardeno TA, Chou SH, Moon HS, Chamberland JP, Fiorenza CG & Mantzoros CS 2010 Leptin in human physiology and therapeutics. *Frontiers in Neuroendocrinology* **31** 377–393. (doi:10.1016/j.yfrne.2010.06.002)

Dempster DW, Compston JE, Drezner MK, Glorieux FH, Kanis JA, Malluche H, Meunier PJ, Ott SM, Recker RR & Parfitt AM 2013 Standardized nomenclature, symbols, and units for bone histomorphometry: a 2012 update of the report of the ASBMR Histomorphometry Nomenclature Committee. *Journal of Bone and Mineral Research* **28** 2–17. (doi:10.1002/jbmr.1805)

Devlin MJ 2011 Why does starvation make bones fat? *American Journal of Human Biology* **23** 577–585. (doi:10.1002/ajhb.21202)

Devlin MJ, Cloutier AM, Thomas NA, Panus DA, Lotinun S, Pinz I, Baron R, Rosen CJ & Bouxsein ML 2010 Caloric restriction leads to high marrow adiposity and low bone mass in growing mice. *Journal of Bone and Mineral Research* **25** 2078–2088. (doi:10.1002/jbmr.82)

Donato J Jr, Cravo RM, Frazao R & Elias CF 2011 Hypothalamic sites of leptin action linking metabolism and reproduction. *Neuroendocrinology* **93** 9–18. (doi:10.1159/000322472)

Dorshkind K, Montecino-Rodriguez E & Signer RA 2009 The ageing immune system: is it ever too old to become young again? *Nature Reviews. Immunology* **9** 57–62. (doi:10.1038/nri2471)

Douyon L & Schteingart DE 2002 Effect of obesity and starvation on thyroid hormone, growth hormone, and cortisol secretion. *Endocrinology and Metabolism Clinics of North America* **31** 173–189. (doi:10.1016/S0889-8529(01)00023-8)

Dubuc PU, Wilden NJ & Carlisle HJ 1985 Fed and fasting thermoregulation in ob/ob mice. *Annals of Nutrition & Metabolism* **29** 358–365. (doi:10.1159/000176992)

Ealey KN, Fonseca D, Archer MC & Ward WE 2006 Bone abnormalities in adolescent leptin-deficient mice. *Regulatory Peptides* **136** 9–13. (doi:10.1016/j.regpep.2006.04.013)

Fantuzzi G & Faggioni R 2000 Leptin in the regulation of immunity, inflammation, and hematopoiesis. *Journal of Leukocyte Biology* **68** 437–446.

Friedman JM & Halaas JL 1998 Leptin and the regulation of body weight in mammals. *Nature* **395** 763–770. (doi:10.1038/27376)

Frystyk J, Skjaerbaek C, Vestbo E, Fisker S & Orskov H 1999 Circulating levels of free insulin-like growth factors in obese subjects: the impact of type 2 diabetes. *Diabetes/Metabolism Research and Reviews* **15** 314–322. (doi:10.1002/(SICI)1520-7560(199909/10)15:5<314::AID-DMRR56>3.0.CO;2-E)

Gat-Yablonski G & Phillip M 2008 Leptin and regulation of linear growth. *Current Opinion in Clinical Nutrition and Metabolic Care* **11** 303–308. (doi:10.1097/MCO.0b013e3282f795cf)

Gennari L, Merlotti D & Nuti R 2011 Aromatase activity and bone loss. *Advances in Clinical Chemistry* **54** 129–164. (doi:10.1016/B978-0-12-387025-4.00006-6)

Gimble JM, Robinson CE, Wu X & Kelly KA 1996 The function of adipocytes in the bone marrow stroma: an update. *Bone* **19** 421–428. (doi:10.1016/S8756-3282(96)00258-X)

Grinspoon SK, Baum HB, Kim V, Coggins C & Klibanski A 1995 Decreased bone formation and increased mineral dissolution during acute fasting in young women. *Journal of Clinical Endocrinology and Metabolism* **80** 3628–3633. (doi:10.1210/jcem.80.12.8530611)

Hamrick MW, Pennington C, Newton D, Xie D & Isales C 2004 Leptin deficiency produces contrasting phenotypes in bones of the limb and spine. *Bone* **34** 376–383. (doi:10.1016/j.bone.2003.11.020)

Hamrick MW, Della-Fera MA, Choi YH, Pennington C, Hartzell D & Baile CA 2005 Leptin treatment induces loss of bone marrow adipocytes and increases bone formation in leptin-deficient *ob/ob* mice. *Journal of Bone and Mineral Research* **20** 994–1001. (doi:10.1359/JBMR.050103)

Hickman J & McElduff A 1990 Insulin sensitizes a cultured rat osteogenic sarcoma cell line to hormones which activate adenylate cyclase. *Calcified Tissue International* **46** 401–405. (doi:10.1007/BF02554971)

Hommel G 1988 A stagewise rejective multiple test procedure based on a modified Bonferroni test. *Biometrika* **75** 383–386. (doi:10.1093/biomet/75.2.383)

Hwa JJ, Ghibaudi L, Compton D, Fawzi AB & Strader CD 1996 Intracerebroventricular injection of leptin increases thermogenesis and mobilizes fat metabolism in *ob/ob* mice. *Hormone and Metabolic Research* **28** 659–663. (doi:10.1055/s-2007-979873)

Inagaki T, Lin VY, Goetz R, Mohammadi M, Mangelsdorf DJ & Kliewer SA 2008 Inhibition of growth hormone signaling by the fasting-induced hormone FGF21. *Cell Metabolism* **8** 77–83. (doi:10.1016/j.cmet.2008.05.006)

Ituarte EA, Ituarte HG & Hahn TJ 1988 Insulin and glucose regulation of glycogen synthase in rat calvarial osteoblast-like cells. *Calcified Tissue International* **42** 351–357. (doi:10.1007/BF02556352)

Iwaniec UT & Turner RT 2013 Failure to generate bone marrow adipocytes does not protect mice from ovariectomy-induced osteopenia. *Bone* **53** 145–153. (doi:10.1016/j.bone.2012.11.034)

Iwaniec UT, Boghossian S, Lapke PD, Turner RT & Kalra SP 2007 Central leptin gene therapy corrects skeletal abnormalities in leptin-deficient *ob/ob* mice. *Peptides* **28** 1012–1019. (doi:10.1016/j.peptides.2007.02.001)

Iwaniec UT, Wronski TJ & Turner RT 2008 Histological analysis of bone. *Methods in Molecular Biology* **447** 325–341. (doi:10.1007/978-1-59745-242-7_2)

Iwaniec UT, Dube MG, Boghossian S, Song H, Helferich WG, Turner RT & Kalra SP 2009 Body mass influences cortical bone mass independent of leptin signaling. *Bone* **44** 404–412. (doi:10.1016/j.bone.2008.10.058)

Jung CH & Kim MS 2013 Molecular mechanisms of central leptin resistance in obesity. *Archives of Pharmacal Research* **36** 201–207. (doi:10.1007/s12272-013-0020-y)

Kim HK & Romsos DR 1990 Adrenalectomy increases brown adipose tissue metabolism in ob/ob mice housed at 35 degrees C. *American Journal of Physiology* **259** E362–E369.

Kimura S, Sasase T, Ohta T, Sato E & Matsushita M 2012 Characteristics of bone turnover, bone mass and bone strength in Spontaneously

http://joe.endocrinology-journals.org
DOI: 10.1530/JOE-14-0224

Published by Bioscientifica Ltd.

Diabetic Torii-*Lepr*^{fa} rats. *Journal of Bone and Mineral Metabolism* **30** 312–320. (doi:10.1007/s00774-011-0324-2)

Kishida Y, Hirao M, Tamai N, Nampei A, Fujimoto T, Nakase T, Shimizu N, Yoshikawa H & Myoui A 2005 Leptin regulates chondrocyte differentiation and matrix maturation during endochondral ossification. *Bone* **37** 607–621. (doi:10.1016/j.bone.2005.05.009)

Kloting N, Koch L, Wunderlich T, Kern M, Ruschke K, Krone W, Bruning JC & Bluher M 2008 Autocrine IGF-1 action in adipocytes controls systemic IGF-1 concentrations and growth. *Diabetes* **57** 2074–2082. (doi:10.2337/db07-1538)

Knehans AW & Romsos DR 1982 Reduced norepinephrine turnover in brown adipose tissue of ob/ob mice. *American Journal of Physiology* **242** E253–E261.

Lindstrom P 2007 The physiology of obese-hyperglycemic mice [*ob/ob* mice]. *ScientificWorldJournal* **7** 666–685. (doi:10.1100/tsw.2007.117)

Luque RM & Kineman RD 2006 Impact of obesity on the growth hormone axis: evidence for a direct inhibitory effect of hyperinsulinemia on pituitary function. *Endocrinology* **147** 2754–2763. (doi:10.1210/en.2005-1549)

Luque RM, Huang ZH, Shah B, Mazzone T & Kineman RD 2007 Effects of leptin replacement on hypothalamic–pituitary growth hormone axis function and circulating ghrelin levels in *ob/ob* mice. *American Journal of Physiology. Endocrinology and Metabolism* **292** E891–E899. (doi:10.1152/ajpendo.00258.2006)

Martineau-Doize B, McKee MD, Warshawsky H & Bergeron JJ 1986 *In vivo* demonstration by radioautography of binding sites for insulin in liver, kidney, and calcified tissues of the rat. *Anatomical Record* **214** 130–140. (doi:10.1002/ar.1092140205)

Menagh PJ, Turner RT, Jump DB, Wong CP, Lowry MB, Yakar S, Rosen CJ & Iwaniec UT 2010 Growth hormone regulates the balance between bone formation and bone marrow adiposity. *Journal of Bone and Mineral Research* **25** 757–768. (doi:10.1359/jbmr.091015)

Mistry AM, Swick AG & Romsos DR 1997 Leptin rapidly lowers food intake and elevates metabolic rates in lean and *ob/ob* mice. *Journal of Nutrition* **127** 2065–2072.

Muller TD, Focker M, Holtkamp K, Herpertz-Dahlmann B & Hebebrand J 2009 Leptin-mediated neuroendocrine alterations in anorexia nervosa: somatic and behavioral implications. *Child and Adolescent Psychiatric Clinics of North America* **18** 117–129. (doi:10.1016/j.chc.2008.07.002)

Munoz MT & Argente J 2002 Anorexia nervosa in female adolescents: endocrine and bone mineral density disturbances. *European Journal of Endocrinology* **147** 275–286. (doi:10.1530/eje.0.1470275)

Myers MG Jr 2004 Leptin receptor signaling and the regulation of mammalian physiology. *Recent Progress in Hormone Research* **59** 287–304. (doi:10.1210/rp.59.1.287)

Naveiras O, Nardi V, Wenzel PL, Hauschka PV, Fahey F & Daley GQ 2009 Bone-marrow adipocytes as negative regulators of the haematopoietic microenvironment. *Nature* **460** 259–263. (doi:10.1038/nature08099)

Pun KK, Lau P & Ho PW 1989 The characterization, regulation, and function of insulin receptors on osteoblast-like clonal osteosarcoma cell line. *Journal of Bone and Mineral Research* **4** 853–862. (doi:10.1002/jbmr.5650040610)

Rafael J & Herling AW 2000 Leptin effect in *ob/ob* mice under thermoneutral conditions depends not necessarily on central satiation. *American Journal of Physiology. Regulatory, Integrative and Comparative Physiology* **278** R790–R795.

Rickard DJ, Iwaniec UT, Evans G, Hefferan TE, Hunter JC, Waters KM, Lydon JP, O'Malley BW, Khosla S, Spelsberg TC *et al.* 2008 Bone growth and turnover in progesterone receptor knockout mice. *Endocrinology* **149** 2383–2390. (doi:10.1210/en.2007-1247)

Robling AG 2012 The interaction of biological factors with mechanical signals in bone adaptation: recent developments. *Current Osteoporosis Reports* **10** 126–131. (doi:10.1007/s11914-012-0099-y)

Saito M & Bray GA 1983 Diurnal rhythm for corticosterone in obese (ob/ob) diabetes (db/db) and gold-thioglucose-induced obesity in mice. *Endocrinology* **113** 2181–2185. (doi:10.1210/endo-113-6-2181)

Solomon G, Atkins A, Shahar R, Gertler A & Monsonego-Ornan E 2014 Effect of peripherally administered leptin antagonist on whole body metabolism and bone microarchitecture and biomechanical properties in the mouse. *American Journal of Physiology. Endocrinology and Metabolism* **306** E14–E27. (doi:10.1152/ajpendo.00155.2013)

Steppan CM, Crawford DT, Chidsey-Frink KL, Ke H & Swick AG 2000 Leptin is a potent stimulator of bone growth in *ob/ob* mice. *Regulatory Peptides* **92** 73–78. (doi:10.1016/S0167-0115(00)00152-X)

Thissen JP, Underwood LE & Ketelslegers JM 1999 Regulation of insulin-like growth factor-I in starvation and injury. *Nutrition Reviews* **57** 167–176. (doi:10.1111/j.1753-4887.1999.tb06939.x)

Thomsen JS, Laib A, Koller B, Prohaska S, Mosekilde L & Gowin W 2005 Stereological measures of trabecular bone structure: comparison of 3D micro computed tomography with 2D histological sections in human proximal tibial bone biopsies. *Journal of Microscopy* **218** 171–179. (doi:10.1111/j.1365-2818.2005.01469.x)

Trayhurn P 1979 Thermoregulation in the diabetic-obese (db/db) mouse. The role of non-shivering thermogenesis in energy balance. *Pflügers Archiv* **380** 227–232. (doi:10.1007/BF00582901)

Trayhurn P & James WP 1978 Thermoregulation and non-shivering thermogenesis in the genetically obese (ob/ob) mouse. *Pflügers Archiv* **373** 189–193. (doi:10.1007/BF00584859)

Trottier MD, Naaz A, Li Y & Fraker PJ 2012 Enhancement of hematopoiesis and lymphopoiesis in diet-induced obese mice. *PNAS* **109** 7622–7629. (doi:10.1073/pnas.1205129109)

Turner RT 1999 Mice, estrogen, and postmenopausal osteoporosis. *Journal of Bone and Mineral Research* **14** 187–191. (doi:10.1359/jbmr.1999.14.2.187)

Turner RT & Iwaniec UT 2011 Low dose parathyroid hormone maintains normal bone formation in adult male rats during rapid weight loss. *Bone* **48** 726–732. (doi:10.1016/j.bone.2010.12.034)

Turner RT, Hannon KS, Demers LM, Buchanan J & Bell NH 1989 Differential effects of gonadal function on bone histomorphometry in male and female rats. *Journal of Bone and Mineral Research* **4** 557–563. (doi:10.1002/jbmr.5650040415)

Turner RT, Riggs BL & Spelsberg TC 1994 Skeletal effects of estrogen. *Endocrine Reviews* **15** 275–300. (doi:10.1210/edrv-15-3-275)

Turner RT, Kalra SP, Wong CP, Philbrick KA, Lindenmaier LB, Boghossian S & Iwaniec UT 2013 Peripheral leptin regulates bone formation. *Journal of Bone and Mineral Research* **28** 22–34. (doi:10.1002/jbmr.1734)

Welch BL 1951 On the comparison of several mean values: an alternative approach. *Biometrika* **38** 330–336. (doi:10.1093/biomet/38.3-4.330)

Westerlind KC, Wronski TJ, Ritman EL, Luo ZP, An KN, Bell NH & Turner RT 1997 Estrogen regulates the rate of bone turnover but bone balance in ovariectomized rats is modulated by prevailing mechanical strain. *PNAS* **94** 4199–4204. (doi:10.1073/pnas.94.8.4199)

Williams GA, Callon KE, Watson M, Costa JL, Ding Y, Dickinson M, Wang Y, Naot D, Reid IR & Cornish J 2011 Skeletal phenotype of the leptin receptor-deficient *db/db* mouse. *Journal of Bone and Mineral Research* **26** 1698–1709. (doi:10.1002/jbmr.367)

Yaturu S 2009 Diabetes and skeletal health. *Journal of Diabetes* **1** 246–254. (doi:10.1111/j.1753-0407.2009.00049.x)

Received in final form 19 June 2014
Accepted 1 July 2014
Accepted Preprint published online 2 July 2014

Published by Bioscientifica Ltd.